TECHNISCHE UNIVERSITÄT WIEN

ATOMINSTITUT

DIPLOMARBEIT

From open-system dynamics to quantum trajectories: Emergent phenomena in many-body systems

zur Erlangung des akademischen Grades

Diplom-Ingenieur

im Rahmen des Studiums

066 461 Technische Physik

eingereicht von

Markus Plautz, BSc
Matrikelnummer: 11901879

ausgeführt am Atominstitut
der Fakultät für Physik der Technischen Universität Wien

Betreuung
Betreuer: **Univ.Prof. Dr. Marcus Huber**

Wien, November 20, 2024

(Unterschrift Verfasser) (Unterschrift Betreuer)

Acknowledgements

First, I would like to thank Marcus for getting the opportunity to write my thesis within his research group and for his time and valuable insights he offered at every discussion since then. I am also especially grateful to Yuri, who has accompanied me on my academic journey from my bachelor thesis on. His insights and our many enlightening discussions have given me a new exciting perspective on the field of physics and have been fundamental to my growth not only as a physicist but also as a person.

I am also deeply thankful to my study colleague and close friend, Niko. His friendship since the first year of university has been invaluable to me and made the challenging early years much more manageable. I also thank my parents and my sister, and close friend, Sabrina, who always encouraged and supported me in the choices I made throughout life.

Finally, I would like to thank my girlfriend, Barbara, for her constant love, friendship, and support. Her caring presence has been a grounding force throughout my studies and without whom this thesis may have taken several more months to finish.

Abstract

In recent years, the study of quantum many-body systems has seen tremendous experimental progress driven by advancements in a variety of platforms initially designed for quantum computing applications. These systems are inevitably subject to decoherence and therefore open system dynamics, which may always be understood as a situation where the environment continuously measures the system and the results are subsequently discarded. On the other hand, when retaining the measurement results, many interesting properties of the system can be accessed. This setting of continuously monitored many-body systems is becoming increasingly feasible in experimental settings.

In this thesis, we study a simplified model of interacting qubits that interpolates between the two extremes of fully retaining or fully discarding the measurement results of the bath. We address the question whether a single measurement trajectory can be distinguished against the backdrop of open-system dynamics by mapping it to a complex "planted" vector Hopfield model. Since the concrete dynamics of our model is fully chaotic, we employ methods from random matrix theory (RMT) to describe it. Using additional tools from quantum information theory, spin glass theory and machine learning, we identify a sharp transition between regimes where a single measurement trajectory can be recovered and those where the system's dynamics are dominated by open-system behavior. This transition bears resemblance to phase transitions in the Hopfield model, where a planted memory may or may not be retrieved.

Zusammenfassung

In den letzten Jahren hat das Studium von Quantenvielteilchensystemen durch Fortschritte in einer Vielzahl von Plattformen, die ursprünglich für Anwendungen in der Quanteninformatik entwickelt wurden, enorme experimentelle Fortschritte erlebt. Diese Systeme sind unvermeidlich Dekohärenz ausgesetzt und unterliegen daher der Dynamik offener Systeme, wobei solche immer als eine Situation verstanden werden kann, in der eine Umgebung das System kontinuierlich misst und die Ergebnisse anschließend verworfen werden. Andererseits erhält man durch das Beibehalten der Messergebnisse Zugang zu vielen interessanten Eigenschaften des Systems. Dieses Szenario der kontinuierlich überwachten Vielteilchensysteme wird in Experimenten zunehmend realisierbar. In dieser Arbeit untersuchen wir ein vereinfachtes Modell interagierender Qubits, welches zwischen den beiden Extremen des vollständigen Beibehaltens oder Verwerfens der Messergebnisse der Umgebung interpoliert. Wir gehen der Frage nach, ob eine einzelne Quantentrajektorie vor dem Hintergrund offener Systemdynamiken unterschieden werden kann, indem wir das Problem auf ein komplexes „planted“ Vektor-Hopfield-Modell abbilden. Da die konkreten Dynamiken unseres Modells vollständig chaotisch sind, verwenden wir Methoden der Random Matrix Theorie (RMT) um diese zu beschreiben. Durch den Einsatz zusätzlicher Werkzeuge aus der Quanteninformationstheorie, der Spinglastheorie und dem maschinellen Lernen identifizieren wir einen scharfen Übergang zwischen den Bereichen, in denen eine einzelne Quantentrajektorie wiederhergestellt werden kann, und jenen, in denen das Verhalten des Systems von offenen Systemdynamiken dominiert wird. Dieser Übergang ähnelt Phasenübergängen im Hopfield-Modell, bei welchem eine Erinnerung möglicherweise wiederhergestellt werden kann oder nicht.

Contents

CHAPTER 1

Introduction

Recent experimental advancements in various experimental platforms that were initially designed for applications in quantum computing, have highlighted the importance of gaining a deeper understanding on the out-of-equilibrium dynamics of quantum many-body systems. Indeed, obtaining more insights into this subject could have profound impact on open questions related to thermalisation, chaos and ergodicity [1, 2].

One particularly active area of research in the study of far-from-equilibrium physics is the field of open quantum systems [3, 4]. In these systems, one is usually interested in the dynamics of only one or a few degrees of freedom, known as the "system", interacting with all remaining degrees of freedom, often referred to as "bath" or "environment". When the environment is assumed to follow certain Markovian assumptions, the resulting dissipative dynamics is well captured by Lindblad operators which obey the celebrated GKLS master equation [5–7].

An especially intriguing aspect of open quantum systems arises when the environment acts as a meter, continuously monitoring the local degrees of freedom of the system throughout its evolution. This combination of quantum gates and subsequent measurements are crucial for various practical applications such as state of the art measurement-based feedback protocols [8] and quantum error correction [9].

One fascinating interpretation of such a setup emerges in cases where measurements are performed, but the outcomes are ultimately discarded, i.e. the meter is left unread. The resulting fundamental lack of knowledge about the state of the system then forces us to describe it as an average over possible measurement outcomes. This "unraveling" of the system's state into an ensemble of pure states represents a common procedure in the context of open system dynamics [10, 11].

A complementary perspective arises when considering continuously monitored systems, where we do have knowledge about the measurement outcomes. Here, the resulting final state of the system will be conditioned on a specific "path" of measurement outcomes and is thus also commonly termed as "quantum trajectory" [12], corresponding to a certain pure state in the unraveling of the system's dynamics.

More recently the notion of quantum trajectories found its way to the many body setting where it led to intriguing new physics, most prominently the theoretical prediction [13, 14] and subsequent experimental discovery [15] of "measurement induced

criticality". In these models, the unitary many-body time evolution of the system is from time to time interrupted by local measurements on a fraction of its degrees of freedom. The resulting competition between unitary dynamics, which generates entanglement, and local projective measurements, which reduce it, then leads to a sharp second-order measurement induced phase transition between regimes of volume-law and area-law entanglement [16, 17].

Within this broader context, a central focus of this thesis is the concept of "retrievability". Here, retrievability refers to the ability to reconstruct the dynamics of an individual quantum trajectory from the noisy backdrop of dissipative open system dynamics. To quantify retrievability, we employ a method analogous to a Principal Component Analysis (PCA) but adapted to the quantum setting. Specifically, the final density matrix of the system is analyzed to extract its largest eigenvalue and the corresponding eigenstate—which essentially corresponds to the first principal component of the system [18, 19]. The overlap between this dominant eigenstate and the specific trajectory of interest is then evaluated. If this overlap is significant, the trajectory is deemed "retrievable", indicating that its dynamics remain detectable despite the contributions of noise and decoherence.

Building on these concepts we just elaborated on, a fundamental question arises: under what conditions can a quantum trajectory be retrieved in the presence of "noisy" dissipative open-system dynamics?

In this thesis, we want to address this question by connecting it to broader themes in physics and machine learning, such as spin glass theory, information retrieval or memory storage. In particular, we introduce a simplified model of interacting spins (or qudits), which interpolates between the two extremes of fully retaining and fully discarding measurement outcomes. Then, in order to perform the aforementioned quantum PCA of our system, we embed this task into a search for the groundstate of an effective spherical spin glass model where our final density matrix takes the place of the random coupling matrix. Furthermore, to make the model and subsequent questions regarding the retrievability of individual trajectories analytically tractable, we will prescribe it with an all-to-all interacting and fully chaotic dynamical evolution. Such dynamics will then allow us to effectively describe the model in terms of random matrix theory (RMT), which poses a powerful tool for calculating analytical properties of such non-integrable systems.

A key result of this work is the identification and quantification of a sharp transition between retrievable and non-retrievable regimes, reminiscent of phase transitions in classical systems like the Hopfield network. We further demonstrate that the eigenvalue spectra of the evolved system provides a clear signature of this transition, offering an intuitive understanding of the retrieval dynamics. However, it should be noted the scope of this work is focused on short-term dynamics, where the evolution of the system is considered over a single timestep. This focus enables analytical tractability and provides a foundation for exploring more complex behavior, including long-term dynamics, in future research.

The structure of this thesis is as follows: Chapter 2 introduces the model and theoretical framework, outlining the mathematical and physical principles underlying quantum trajectories and open-system dynamics. Chapter 3 presents the main results, demonstrating the emergence of a retrievable phase and connecting these findings to insights from machine learning and spin glass theory. Chapter 4 provides conclusions and a discussion of future research directions. Finally, detailed derivations and supplementary analyses are provided in the appendices for interested readers.

CHAPTER 2

Model and framework

In this chapter we introduce the general setup of our model and give a quick overview of its theoretical preliminaries.

2.1 Introduction to the model

Consider a lattice (circuit) model in $1+1$ dimensions represented by a chain of l qudits where the dynamics are given by a Floquet like time evolution that is discrete in time $t \in \mathbb{Z}$. At each individual time step the lattice is evolved by a unitary operator U which is typically given by a tensor product of local unitary gates acting on pairs of qudits (Fig. 2.1a). In our model we will relax this constriction of spatial locality and instead consider dynamics that is described by an all-to-all coupling between the qudits (Fig. 2.1b). To consider open system dynamics, we divide our l qudits into n system and p environment or "ancilla" qudits such that $n+p=l$. Noting that each individual qudit carries a local Hilbert state space of dimension d, the total Hilbert space dimension of the system

(a) (b)

Figure 2.1: (a) Example of a spatially local quantum circuit, such an architecture is also referred to as a "brickwork" circuit in the literature. Each leg corresponds to an individual qudit while blue rectangles depict unitary gate that act on the Hilbert space of the incoming legs. By thinking of this structure in terms of a Trotterized many-body system, one can interpret it as universal approximation of a system with nearest-neighbor interactions [20]. (b) All-to-all interacting unitary circuit. In the past, this model has found many interesting applications, an example being the study of scrambling in black holes if the individual gates are sampled from the unitary Haar measure [21, 22].

is given by $N = \dim(\mathcal{H}_S) = d^n$ while that of the environment is $P = \dim(\mathcal{H}_E) = d^p$. Additionally, we want to define the quantity

$$\alpha = \frac{P}{N}, \tag{2.1.1}$$

which will prove to be useful in the remaining part of the thesis. As illustrated in Fig. 2.1, the time evolution of the circuit will be given a sequence of t unitary operators U that couple all l qudits of the lattice simultaneously. Due to their analytical tractability, we will focus on unitary gates that are sampled from the Haar measure on $\mathrm{U}(NP)$, meaning that $U = U_{\mathrm{Haar}}$ for this work.

2.1.1 Quantum trajectories

Suppose now that after each individual time step we perform a generalized measurement on the system. To do so, we introduce a positive operator-valued measure (POVM) which, using Naimark's dilation theorem, can also be regarded as projective measurement on a larger Hilbert space. In this sense, the enlarged Hilbert space is characterized by the space of all l qudits and the projective measurements are performed on the qudits of the environment while storing the associated measurement outcomes after each timestep m_j in the tuple $\boldsymbol{m} = (m_1, m_2, \ldots, m_t)$. Assuming that our initial state is described by a product state of our system ρ_S and the environment $\rho_E = |0\rangle\langle 0|$, one then readily obtains the post measurement state of the system by performing a partial trace over the environment of the joint evolved system, i.e. we can write (without normalization)

$$\mathcal{E}[\rho_S]_{\boldsymbol{m}} \propto \mathrm{tr}_E\left(E_{\boldsymbol{m}}\left(\rho_S \otimes |0\rangle\langle 0|\right) E_{\boldsymbol{m}}^\dagger\right), \tag{2.1.2}$$

where

$$E_{\boldsymbol{m}} = P_{m_t} U_t \cdots P_{m_2} U_2 P_{m_1} U_1, \tag{2.1.3}$$

with the projection operators being defined in the usual way as

$$P_{m_j} = \mathrm{I}_N \otimes |m\rangle\langle m|, \quad \text{with} \quad \{|m\rangle\}_{m=0}^{P-1}. \tag{2.1.4}$$

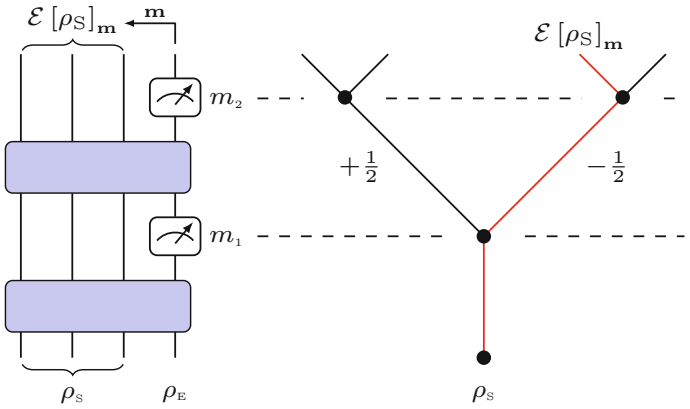

Figure 2.2: Illustrative example of the concept of quantum trajectories. For simplicity, we consider an environment consisting of only one qubit ($d = 2$). The projective measurements are performed on the z-component of the qubit and yield either $+1/2$ or $-1/2$. Due the probabilistic nature of the measurement process, every new experimental run could result in a different trajectory describing $\rho_{\boldsymbol{m}}$. One exemplary sequence of outcomes corresponding to $\boldsymbol{m} = (-1/2, +1/2)$ is highlighted by the red path.

The post measurement state $\mathcal{E}[\rho_S]_{\boldsymbol{m}}$ now represents what is known as a "quantum trajectory" in the literature [12, 23]. In this context, the word trajectory refers to the path of measurement outcomes that characterize a certain post measurement state conditioned on $\boldsymbol{m}$, see Fig. 2.2 for an example [11].

In order to fully describe the normalized state of the system conditioned on the measurement outcome $\boldsymbol{m}$, we now introduce the Kraus operator

$$A_{\boldsymbol{m}} \equiv \langle m | U_t \dots P_{m_2} U_2 P_{m_1} U_1 | 0 \rangle, \tag{2.1.5}$$

which allows us to write the channel as

$$\mathcal{E}[\rho_S]_{\boldsymbol{m}} = \frac{A_{\boldsymbol{m}} \rho_S A_{\boldsymbol{m}}^\dagger}{p_{\boldsymbol{m}}}, \tag{2.1.6}$$

where the normalization constant $p_{\boldsymbol{m}} = \mathrm{tr}\left(A_{\boldsymbol{m}} \rho_S A_{\boldsymbol{m}}^\dagger\right)$ corresponds to the probability of obtaining a certain trajectory $\boldsymbol{m}$.

2.1.2 Dissipative information loss

So far we have only considered the situation where, upon performing a sequence of measurements on the circuit, we always keep perfect track of each individual measurement outcome which allowed us to fully specify the post measurement of the system. This situation changes if we consider scenario in which we discard all the measurement results such that we have no knowledge about the specific outcomes. Such an intrinsic lack of information forces us describe the post measurement state $\tilde{\rho}$ as a statistical mixture of all possible quantum trajectories, i.e. we have

$$\mathcal{E}[\rho_S] = \mathbb{E}\left[\mathcal{E}[\rho_S]_{\boldsymbol{m}}\right] = \sum_{\boldsymbol{m}} p_{\boldsymbol{m}} \mathcal{E}[\rho_S]_{\boldsymbol{m}}\,. \tag{2.1.7}$$

Considering that an individual trajectory is given by Eq. (2.1.6), we can rewrite this state to

$$\mathcal{E}[\rho_S] = \sum_{\boldsymbol{m}} A_{\boldsymbol{m}} \rho_S A_{\boldsymbol{m}}^\dagger, \tag{2.1.8}$$

where, due to the trace preserving condition, the Kraus operators have to fulfill the condition that $\sum_{\boldsymbol{m}} A_{\boldsymbol{m}}^\dagger A_{\boldsymbol{m}} = \mathrm{I}_N$. For the dynamics that we consider in this thesis, this state will always tend to the maximally mixed (i.e. infinite temperature) state after a sufficient amount of time. Note that the description of this state would be equivalent to a situation where, instead of considering measurements on the environment, we have decoherence of the system state due to an interaction with some uncontrolled bath.

2.1.3 Model setup

As already stated in Chapter 1, our goal is to unravel the connections between the setting of a dissipative system undergoing decoherence due to an uncontrolled interaction with an environment and a system that is continuously monitored and where we always have perfect knowledge about the outcomes of the measurements. To do so, we introduce a model where we interpolate between those two settings with an interpolation parameter $\eta \in [0, 1]$ such that the evolved state of the system is described by

$$\rho(t+1) = \eta \mathcal{E}[\rho(t)]_{\boldsymbol{m}} + (1-\eta)\,\mathcal{E}[\rho(t)]\,, \tag{2.1.9}$$

meaning that the parameter η can be seen as the probability that we keep track of the measurement outcomes at time t. Note that the density matrix ρ does not explicitly carry an index $\mathbf{m}$, this results from an independence of the specific "unraveling" of our model. This argument will be justified later on in Section (3.2).

Instead of considering the model for arbitrary long times, however, we will focus on the case where the dynamics is given by only one single time step. In this case, the Kraus operators from Eq. (2.1.5) simplify to

$$A_m = \langle m|U|0\rangle, \tag{2.1.10}$$

where we note that our previously defined tuple of measurement outcomes $\boldsymbol{m}$ now reduced to the single outcome m obtained after the first time step. In this context, our above defined model reduces to

$$\rho = \eta\mathcal{E}\left[\rho_S\right]_m + (1-\eta)\,\mathcal{E}\left[\rho_S\right]. \tag{2.1.11}$$

2.2 RMT model of the dynamics

In its present form, it is hard to analyze general properties of the model proposed in Eq. (2.1.11). For this reason, we will instead consider an effective RMT model where we replace the Kraus operator defined in Eq. (2.1.10) by

$$A_n = \frac{G_n}{\sqrt{NP}}, \tag{2.2.1}$$

with the entries of the $N \times N$-dimensional complex matrix G_n being given by

$$(G_n)_{ij} \overset{\text{i.i.d}}{\sim} \frac{1}{\sqrt{2}}\left(\mathcal{N}(0,1) + i\mathcal{N}(0,1)\right), \tag{2.2.2}$$

where the notation $\mathcal{N}(0,1)$ denotes a normal distributed random variable with mean 0 and variance 1.

Random matrices defined this way are known as complex Ginibre matrices in the literature [24]. The justification for Eq. (2.2.1) follows from a well known result from the study of large Haar distributed unitary matrices, stating that *any* $k \times k$ submatrix of a random $n \times n$ unitary matrix converges to a matrix of independent complex Gaussian random variables with mean 0 and variance 1 in the limit where $n \to \infty$ and after multiplying it with a normalization factor equal to $\sqrt{n}$ [25, 26]. For our model, this implies that the effective RMT model becomes exact in the thermodynamic limit where the number of qudits $l \to \infty$. Since the eigenvalues of a complex Ginibre matrix are confined to the unit disc, a result known as circular law [24], we expect the radius of $G_n/\sqrt{NP}$ to be equal to $1\sqrt{P}$ (see Fig. 2.3).

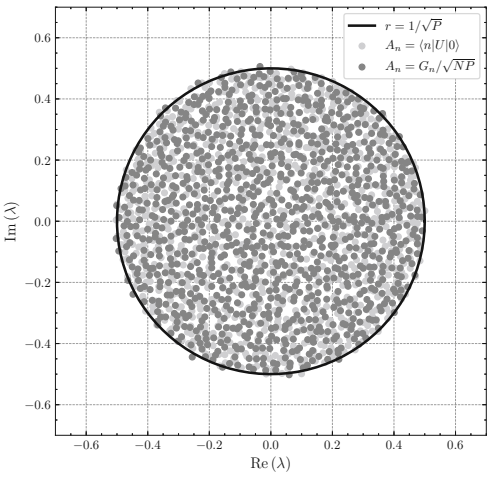

Figure 2.3: Eigenvalues of a truncated Haar-unitary matrix (silver) and an effective Kraus operator described by RMT (gray) for $N = 1024$ and $P = 4$.

Let us now validate the use of these Kraus operators by checking if they fulfill the necessary conditions to describe a valid POVM, i.e. we need to show that

$$A_n^\dagger A_n \geq 0, \ \forall n \quad \text{and} \quad \sum_{n=1}^{P} A_n^\dagger A_n = \mathrm{I}_N. \tag{2.2.3}$$

The first condition can be shown easily by noting that the eigenvalues of the operator $A_n^\dagger A_n$ follow a Wishart distribution [27], hence making it necessarily a positive semi-definite operator. The second condition, however, does not hold in general. Nonetheless, one can show that the condition is fulfilled at least on *average*, i.e. that (see Appendix A.1.1)

$$\mathbb{E}\left[M\right] = \mathrm{I}_N, \quad \text{with} \quad M = \sum_{n=1}^{P} A_n^\dagger A_n. \tag{2.2.4}$$

To check how this result fluctuates on average, we calculate the variance which results in (check again Appendix A.1.1 for detailed steps)

$$\mathrm{Var}\left[M\right] = \mathbb{E}\left[M^2\right] - \left(\mathbb{E}\left[M\right]\right)^2 = \frac{q}{N}\mathrm{I}_N, \tag{2.2.5}$$

showing that the POVM defined by the elements $\left\{A_n^\dagger A_n\right\}$ is self-averaging, i.e. there is a concentration of measure in the thermodynamic limit $N \gg 1$. We conclude that in this limit already a single realization of the channel describes a valid POVM.

2.2.1 Quantum trajectory with random operators

We now want to investigate the quantum trajectory produced by our random Kraus operators. Because of the disorder, we are particularly interested in the mean updated state given by $\mathbb{E}\left[\mathcal{E}\left[\rho_\mathrm{S}\right]_m\right]$ where $\mathcal{E}\left[\rho_\mathrm{S}\right]_m$ is defined in the usual way (see Eq. (2.1.6)). Dealing with this quantity analytically, however, can become very challenging since the term in the denominator will usually fluctuate heavily for a small total Hilbert space dimension NP. We thus want to investigate the quantity $\mathbb{E}\left[p_m\right]$ and see how it behaves in the thermodynamic limit. Doing the average (see Appendix A.2.1) gives us

$$\mathbb{E}\left[p_m\right] = \frac{1}{P}, \tag{2.2.6}$$

while the variance is given by

$$\mathrm{Var}\left[p_m\right] = \mathbb{E}\left[p_m^2\right] - \left(\mathbb{E}\left[p_m\right]\right)^2 = \frac{q^2}{N^3}. \tag{2.2.7}$$

This shows us that for large system sizes, $N \gg 1$, the quantity p_m is self-averaging, allowing us to replace

$$p_m \overset{N\gg 1}{\longrightarrow} P^{-1}. \tag{2.2.8}$$

Thus, assuming that our initial system state starts out in the pure state $\rho_\mathrm{S} = |0\rangle\langle 0|$, the updated state becomes

$$\mathcal{E}\left[\rho_\mathrm{S}\right]_m = \frac{A_m \rho_S A_m^\dagger}{P^{-1}} = \frac{1}{N}\sum_{i,j=1}^{N} G_{m,i0} G_{m,0j}^\dagger |i\rangle\langle j| = |\psi^{(m)}\rangle\langle\psi^{(m)}|, \tag{2.2.9}$$

where we defined

$$|\psi^{(m)}\rangle = \sum_{i=1}^{N} c_{m,i}|i\rangle, \quad \text{with} \quad c_{m,i} = \frac{G_{m,i0}}{\sqrt{N}}. \tag{2.2.10}$$

One should note that this state is, in general, not properly normalized. But since we are anyway only interested in the average, we can take a look at the distribution of the squared norm of this quantity. Doing a simple calculation reveals (check Appendix A.2.2 for details)

$$\mathbb{E}\left[\langle\psi|\psi\rangle\right] = 1. \tag{2.2.11}$$

While the fluctuations around this result are given by

$$\mathrm{Var}\left[\langle\psi|\psi\rangle\right] = \mathbb{E}\left[\langle\psi|\psi\rangle^2\right] - \left(\mathbb{E}\left[\langle\psi|\psi\rangle\right]\right)^2 = \frac{1}{N}, \tag{2.2.12}$$

showing again that the distribution of the squared norm concentrates around a normalized state vector $|\psi\rangle$ for $N \gg 1$.

2.2.2 Dissipative channel with random operators

Now that we have dealt with the description of quantum trajectories in terms of random Kraus operators, we want to turn our attention on the dissipative part of Eq. (2.1.11). What we can show is, that the eigenvalue distribution for this term will follow a Marčenko-Pastur distribution [28]. To see this, we perform the following computation

$$\begin{aligned}
\mathcal{E}\left[\rho_S\right] &= \sum_{n=1}^{P} A_n \rho_S A_n^\dagger = \frac{1}{NP}\sum_{n=1}^{P} G_n \rho_S G_n^\dagger \\
&= \frac{1}{NP}\sum_{i,j=1}^{N}\sum_{n=1}^{P} |i\rangle\langle i|G_n|0\rangle\langle 0|G_n^\dagger|j\rangle\langle j| \\
&= \frac{1}{NP}\sum_{i,j=1}^{N}\left(\sum_{n=1}^{P} G_{n,i0}G_{n,j0}^*\right)|i\rangle\langle j| \\
&= \frac{1}{N}\sum_{i,j=1}^{N}\frac{1}{P}\left(\mathcal{G}\mathcal{G}^\dagger\right)_{ij}|i\rangle\langle j|,
\end{aligned} \tag{2.2.13}$$

where we defined the $N \times P$ dimensional matrix

$$\mathcal{G}_{ij} = G_{i,j0}, \quad \text{with} \quad 1 \le i \le N, 1 \le j \le P, \tag{2.2.14}$$

whose elements are of course still distributed according to Eq. (2.2.2).

By recalling that the Wishart matrix for a dataset of P, N-dimensional random data vectors x_n is nothing but the sample covariance matrix defined as $\mathbf{W} = \sum_{n=1}^{P} \mathbf{x}_n\mathbf{x}_n^\top/P = \mathbf{X}\mathbf{X}^\top/P$, we can finally write

$$\mathcal{E}\left[\rho_S\right] = \sum_{n=1}^{P} A_n \rho_S A_n^\dagger = \frac{1}{N}\sum_{i,j}^{N}\tilde{\mathcal{W}}_{ij}|i\rangle\langle j|. \tag{2.2.15}$$

Combining this result with the effective quantum trajectory obtained in Eq. (2.2.9) finally allows us to write our effective model as

$$\rho = \eta|\psi\rangle\langle\psi| + (1-\eta)\,\mathcal{W}, \quad \text{where} \quad \mathcal{W} = \frac{1}{N}\tilde{\mathcal{W}}. \tag{2.2.16}$$

Observe the two different contributions to the spectrum of ρ. On one hand, if we concentrate on the extreme case $\eta = 0$, as already mentioned, the spectrum will be distributed according to the famous Marčenko-Pastur distribution. With $\eta = 1$, however, the spectrum will be described by the eigenvalues of the pure state describing a certain quantum trajectory, meaning that we have a single eigenvalue equal to 1 while all others are 0. Accordingly, for values of η in between these two extreme cases, the distribution will be described by a mixture of these two. One can therefore expect, that after crossing a certain critical value η_c, the single peak produced by the pure state will start to emerge out of the Marčenko-Pastur "bulk" while essentially staying "hidden" if kept below this value. In fact, such a transition can not only be observed by varying the parameter η, see Fig. 2.4 below, but also by variation of the size of the bath through the parameter α. Observing the transition by sweeping over this parameter describes what is known as a Baik-Ben Arous-Péché (BBP) phase transition in the literature [29].

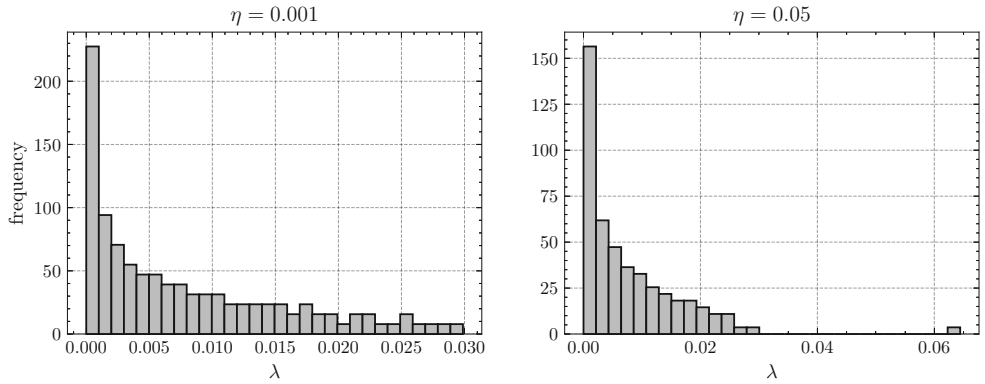

Figure 2.4: The eigenvalues λ of ρ for different values of η. The dimension of the system and the environment are both equal to $N = P = 128$. We see a clear separation from the bulk of the Marčenko-Pastur distribution for high enough values of η. The moment this peaks disappears in the bulk of the noise indicates roughly the critical point where we lose the ability to reconstruct the original dynamics of a single trajectory.

CHAPTER 3

Main results

Now that the main setup of our model has been established, we now want to turn our attention to the main question of this thesis, that is, we want to ask for what strength of the dissipative part of our model (Eq. (2.2.16)) are we still able to recover the dynamics defined by the quantum trajectory $|\psi\rangle$.

We can expect that for large values of η, the eigenvector $|0\rangle$ of ρ associated with the largest eigenvalue will be very close to the state $|\psi\rangle$. For smaller values, however, the state $|0\rangle$ should start to mix with the eigenvectors of the bulk produced by the Wishart matrix $\mathcal{W}$, implying that the overlap of $|0\rangle$ with $|\psi\rangle$ will begin to shrink. In what follows we are thus motivated to find an analytical expression for the quantity

$$m^2 = |\langle 0|\psi\rangle|^2. \tag{3.0.1}$$

To accomplish this task, we will build up a connection to a well studied problem in machine learning theory that we want to discuss in the following Section.

3.1 Connections to machine learning theory and spin glasses

Unsupervised learning is a branch of machine learning whose goal is to find hidden structures or patterns in a given dataset. The term "unsupervised" emphasizes, that the model, say a neuronal network, has to find this structure itself, i.e. there is no feedback whatsoever from some outside entity whether the resulting output is correct. This differs to the branch of supervised learning where such feedback is present.

Suppose now we are dealing with a dataset that has such a hidden structure, how would we go about finding it? Let us assume that the dataset has N observations each for a total set of P variables, we label the vector containing the N observations as $\boldsymbol{\xi}_\mu \in \mathbb{R}^N$, where μ labels the specific variable we are looking at, i.e. $\mu = 1, \dots, P$. The usual strategy now is, see [30–32] and references therein, to seek for an optimal "retrieval configuration" $\boldsymbol{v} \in \mathbb{R}^N$, such that the overlap between observed data and this vector, i.e.

$$\lambda_\mu = \frac{1}{\sqrt{N}} \mathbf{v} \cdot \boldsymbol{\xi}_\mu, \tag{3.1.1}$$

is such that it minimizes a certain energy function that we write as

$$E(\mathbf{v}) = \sum_{\mu=1}^{P} V(\lambda_\mu), \tag{3.1.2}$$

with the potential $V(\lambda_\mu)$.

Note that we included an additional factor $1/\sqrt{N}$ in Eq. (3.1.1), in many applications of unsupervised learning the data vector $\boldsymbol{\xi}_\mu$ is assumed to be sampled from a standard normal distribution, meaning that its length approaches $\sqrt{N}$ in the limit for large N [33]. It is therefore convenient to also normalize other N-dimensional vectors such that their length is equal to $\sqrt{N}$. This implies that the minimization of the energy function $E(\mathbf{v})$ has the additional constraint that $\mathbf{v}^2 = N$.

To proceed, one now has to specify the potential $V(\lambda_\mu)$, essentially determining what kind of unsupervised learning algorithm will be used. Take, for example, the linear potential $V(\lambda_\mu) = -\lambda_\mu$. In this case, $\mathbf{v}$ will point along the mean (or center-of-mass) vector of the dataset, since, in order to minimize the energy, it will necessarily be given by $\mathbf{v} \propto \sum_\mu \boldsymbol{\xi}_\mu$. In the literature, this specific algorithm is referred to as Hebbian learning [34].

Another useful choice we can make for the function $V(\lambda_\mu)$ is that of a quadratic potential, i.e. where

$$V(\lambda_\mu) = -\lambda_\mu^2. \tag{3.1.3}$$

In this case, the learning algorithm is known as Oja's rule [35] or maximal variance learning (i.e. principal component analysis). Here, the energy function takes the form

$$E(\mathbf{v}) = -\frac{1}{N}\sum_{\mu=1}^{P} \mathbf{v}^\top \boldsymbol{\xi}_\mu \boldsymbol{\xi}_\mu^\top \mathbf{v} = -\frac{1}{N}\mathbf{v}^\top C \mathbf{v}, \tag{3.1.4}$$

where $C = \sum_\mu \boldsymbol{\xi}_\mu \boldsymbol{\xi}_\mu^\top$ is defined as the sample covariance matrix of the data. In this form, it also becomes evident why this choice of potential is known as maximal variance learning. Namely, in order to minimize the given energy, the vector $\mathbf{v}$ will necessarily point along the direction of the eigenvector corresponding to the maximal eigenvalue of the covariance matrix C. This, of course, is equivalent to saying that $\mathbf{v}$ points along the first principal component of the $N \times P$-dimensional data matrix X whose columns are given by $\boldsymbol{\xi}_\mu$.

Let us now return to our problem statement and see how we can map it to the framework we just elaborated on. As already stated in Equation (3.0.1), we are interested in calculating the overlap between the eigenvector corresponding to the largest eigenvalue of ρ and the state $|\psi\rangle$. In order to retrieve this quantity, we employ the method of maximal variance learning and define the quadratic energy function

$$E(\mathbf{v}) = -\mathbf{v}^\dagger \rho \mathbf{v}, \tag{3.1.5}$$

where we replaced the transpose with the dagger operation since in our setting $\mathbf{v} \in \mathbb{C}^N$. Written in this form, it becomes evident that our problem can be mapped to the spherical Sherrington-Kirkpatrick (SSK) spin glass model [36] whose Hamiltonian is given by

$$E(\mathbf{v}) = -\frac{1}{\sqrt{N}}\sum_{i,j} J_{ij} v_i v_j, \tag{3.1.6}$$

where we identified the coupling matrix with $J = \rho/\sqrt{N}$. Spherical in this context refers to the property of the system that the spins are confined to the $N-1$-dimensional sphere $\mathbb{S}^{N-1}\left(\sqrt{N}\right) = \left\{\mathbf{v} \in \mathbb{R}^N : \mathbf{v}^2 = N\right\}$ instead of a lattice $\mathbf{v} = \{-1, 1\}^N$ as in the usual Sherrington-Kirkpatrick (SK) model [37].

Recall that we asserted that in the extreme case of a purely dissipative channel, $\eta = 0$, the distribution of the eigenvalues of ρ and thus of the couplings will follow a Marčenko-Pastur distribution. For the more general case of $\eta \neq 0$, however, the distribution will be modified according to a "spiked"-Wishart model [29], where in our case the "spike" is given by a rank 1 perturbation.

This perturbation can also be seen as a kind of "planted" memory if one views the energy function in Eq. (3.1.6) through the lens of a vectorized "planted" Hopfield model [38]. In this model, memory patterns are stored as stable attractors in its energy landscape. When presented with a partial or noisy input pattern, the network aims to evolve toward the nearest attractor, thus retrieving a stored memory. Of course this also applies to the setting of spin glasses. Here, configurations can settle into various stable states depending on the degree of disorder of the coupling matrix J. By analyzing the overlap between configurations, we can assess whether the system is in a "retrievable" phase, dominated by a single coherent trajectory, or in a "non-retrievable" phase where the state is effectively randomized by decoherence.

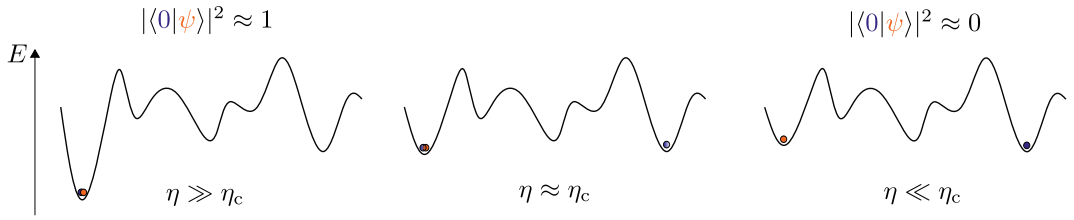

Figure 3.1: Energy landscape of a Hopfield network or spin glass model with a certain "planted" configuration $|\psi\rangle$. In our model, the disorder is varied via the efficiency parameter η. For values of η above a certain critical value η_c, we observe a strongly pronounced minima of the energy landscape which enables the ground state $|0\rangle$ to condense onto it. With η close to the critical value we observe a smoothening of the energy landscape such that there are many equally likely configurations of the system. For η far below the critical value the spike disappears in the bulk of the noise matrix, leading to a condensation of the system to a false minimum. In the context of Hopfield networks, these false minima are called spurious attractors.

To retrieve the overlap parameter, which is nothing but the mean magnetization in the context of spin glasses, we now define the Gibbs distribution associated to the energy function Eq. 3.1.5 as

$$p(\mathbf{v}, \beta) = \frac{1}{Z} e^{-\beta E(\mathbf{v})}, \tag{3.1.7}$$

with the "inverse temperature" β and the partition function Z which is defined in the usual way as

$$Z = \int \mathrm{d}\mathbf{v} e^{-\beta E(\mathbf{v})}. \tag{3.1.8}$$

Note that as $\beta \to \infty$, the Boltzmann weight $\exp\left[-\beta E(\mathbf{v})\right]$ becomes increasingly peaked at the configuration $\mathbf{v}$ that minimizes $E(\mathbf{v})$, corresponding to the ground state of the system. In this limit, the partition function effectively isolates the dominant eigenstate of the

system's density matrix, which aligns with the quantum PCA-inspired analysis employed in this work. This process is often referred to as Boltzmann-Gibbs regularization, as it filters out contributions from higher-energy states and focuses solely on the ground state.

In the context of this thesis, the ground state corresponds to the eigenvector associated with the largest eigenvalue of the density matrix. The overlap between this dominant eigenvector and the quantum trajectory of interest quantifies the "retrievability" of the trajectory. In the following Section we want to concentrate our efforts on obtaining the partition function of the system in order to extract this overlap out of it.

3.2 Computing the overlap

Let us come back to our model defined in Eq. (2.2.16). As a first step, it will prove useful to write it back into its original form where we had

$$\rho = \eta \frac{A_m \rho A_m^\dagger}{p_m} + (1-\eta) \sum_{\mu=1}^{P} A_\mu \rho A_\mu^\dagger. \tag{3.2.1}$$

Note now that trajectory which we want to recover is also present in the "noise" on the right-hand side. Pulling the term where $\mu = m$ out of the sum and writing $p_k = P^{-1}$ while also using the random matrix representation of A_m since we are interested in the limit for large N and P, then allows us to write

$$\rho = \frac{a_\eta}{N} \mathbf{g}_m \mathbf{g}_m^\dagger + \frac{(1-\eta)}{NP} \sum_{\mu \neq m}^{P} \mathbf{g}_\mu \mathbf{g}_\mu^\dagger,$$

where we defined the N-dimensional vector $G_{m,i0} = (\mathbf{g}_m)_i$ and the rescaled parameter

$$a_\eta = \frac{(1 + \eta\,(P-1))}{P}. \tag{3.2.2}$$

Given that the sum over all trajectories now only contains $P-1$ terms, we renormalize it through a multiplication by

$$\rho = \frac{a_\eta}{N} \mathbf{g}_m \mathbf{g}_m^\dagger + \frac{b_\eta}{P-1} \sum_{\mu \neq m}^{P} \mathbf{g}_\mu \mathbf{g}_\mu^\dagger,$$

where now

$$b_\eta = \frac{(1-\eta)\,(P-1)}{NP}. \tag{3.2.3}$$

Using the fact that the spectrum of ρ is invariant under unitary transformations, we then define a unitary operator U such that the transformation $\rho \to U\rho U^\dagger$ gives us the simple form $\mathbf{u} = U\mathbf{g}_m = \left(\sqrt{N}, 0, \ldots, 0\right)^\top \in \mathbb{R}^N$, where the factor $\sqrt{N}$ ensures that the length of $\mathbf{g}_m$ stays the same. This makes it also apparent why the specific "unraveling" of the trajectory does not matter, and we are free to choose any convenient one. We thus end up with the final model

$$\rho = \frac{a_\eta}{N} \mathbf{u}\mathbf{u}^\dagger + \frac{b_\eta}{P-1} \sum_{\mu=1}^{P-1} \mathbf{g}_\mu \mathbf{g}_\mu^\dagger. \tag{3.2.4}$$

To additionally demand that the sampled vector $\mathbf{v}$ has the property $\mathbf{v}^2 = N$, we add a constraint to the energy function such that

$$E(\mathbf{v}, \rho) = -\frac{1}{2}\mathbf{v}^\dagger \rho \mathbf{v} + \frac{z}{2}\left(\mathbf{v}^\dagger \mathbf{v} - N\right), \tag{3.2.5}$$

where the scalar quantity z acts as a Lagrange multiplier and a factor of $1/2$ was added for convenience.

With our energy at hand, we now define the Helmholtz free entropy in the usual way as

$$\Phi = \lim_{N\to\infty} \Phi_N, \tag{3.2.6}$$

where Φ_N is called the free entropy density being given by

$$\Phi_N = -\frac{2}{N}\log\left[Z(\rho)\right] = -\frac{2}{N}\log\left[\int \mathrm{d}\mathbf{v}\; e^{-\beta E(\mathbf{v},\rho)}\right], \tag{3.2.7}$$

where we included a non-conventional prefactor of 2 in order to simplify our calculations later on.

It is now crucial to remark that, through its dependence on the partition function and thus ρ, the free entropy itself will be subject to randomness. For this reason, computing Φ_N alone will only give us the free entropy for a specific realization of the disorder. Luckily, however, the free entropy density has the very nice property that it is self-averaging, a concept we already encountered in the previous Chapter. What it means is, that for all kind of different realization of the disorder and in the limit for very large system sizes N, Φ_N will concentrate on its average value. Thus, in order to study our system in the thermodynamic limit, it suffices to compute

$$\mathbb{E}\left[\Phi_N\right] = -\frac{1}{N}\mathbb{E}\left[\log\left[Z(\rho)\right]\right], \tag{3.2.8}$$

where the averaging is performed with respect to the disorder present in ρ. In the literature, the above quantity is also commonly referred to as the quenched average of the system.

The challenge one now faces is, that besides computing the partition function on its own, which by all means is also a highly non-trivial task, computing the average of the logarithm of this quantity is usually much more complicated and often not analytically tractable. Luckily, there exists a very nice method known as the replica method that will us to circumvent the problem of computing the average of the logarithm.

3.2.1 The replica method

The basic argument of the replica method goes as follows. Suppose n is very close to zero, then

$$Z^n = e^{n\log(Z)} = 1 + n\log(Z) + \mathcal{O}\left(n^2\right), \tag{3.2.9}$$

which implies that

$$\log(Z) = \lim_{n\to 0}\frac{Z^n - 1}{n},$$

leaving us with the final result that

$$\mathbb{E}\left[\log(Z)\right] = \lim_{n\to 0}\frac{\mathbb{E}\left[Z^n\right] - 1}{n}. \tag{3.2.10}$$

The scheme for this calculation is now to first assume that $n \in \mathbb{N}$, obtain the corresponding average of Z^n and then perform an analytical continuation for $n \to 0$. There is, however, a problem with this approach since nothing can guarantee us the validity of this last step, and we often have to hope that the correct result can be actually obtained this way. Still, as of today, there is a strong trust in the replica method since it always seemed to retrieve the same result that could be obtained by rigorous computations. One example of this was the seminal work of Giorgio Parisi in which he showed that the SK spin glass model could be solved exactly by the replica method if one assumes something that is known as "replica symmetry breaking" [39]. It was this insight and a number of other important contributions for which he was ultimately awarded the Nobel Prize in physics in 2021.

We now want to return to our calculation. As stated above, we first assume that $n \in \mathbb{N}$. This way, the average over Z^n can be interpreted as the expectation value of n non-interacting copies of our system. Written down explicitly it reads

$$\begin{aligned}\mathbb{E}_\rho\left[Z\left(\rho\right)^n\right] &= \mathbb{E}_\rho\left[\left(\int \mathrm{d}\mathbf{v}\ e^{-\beta E(\mathbf{v},\rho)}\right)^n\right] \\ &= \mathbb{E}_\rho\left[\int \prod_{\alpha=1}^{n} \mathrm{d}\mathbf{v}^{(\alpha)}\ e^{-\beta E\left(\mathbf{v}^{(\alpha)},\rho\right)}\right],\end{aligned}$$

where we labeled each individual copy of the system by the index α.

Given that the expectation is performed over the disorder contained in ρ, which is realized by the complex Ginibre random matrix $\mathbf{G}$, we can now move the average to the relevant parts of the equation to obtain

$$\begin{aligned}\mathbb{E}_\rho\left[Z\left(\rho\right)^n\right] = \int \prod_{\alpha=1}^{n} \mathrm{d}\mathbf{v}^{(\alpha)}\ \exp\left\{-\frac{z}{2}\left(\mathbf{v}^{(\alpha)\dagger}\mathbf{v}^{(\alpha)} - nN\right) + \frac{a_\eta}{2N}\mathbf{v}^{(\alpha)\dagger}\mathbf{u}\mathbf{u}^\dagger\mathbf{v}^{(\alpha)}\right\} \\ \mathbb{E}_{\mathbf{G}}\left[\exp\left\{\frac{b_\eta}{2\left(P-1\right)}\sum_{\alpha=1}^{n}\sum_{\mu=1}^{P-1}\mathbf{v}^{(\alpha)\dagger}\mathbf{g}_\mu\mathbf{g}_\mu^\dagger\mathbf{v}^{(\alpha)}\right\}\right],\end{aligned} \tag{3.2.11}$$

where we gave each copy of $\mathbf{v}$ an index α.

Given that the average over $\mathbf{G}$ is simply given by a Gaussian integral, we can show that it leads to (Appendix B.1.1)

$$\begin{aligned}\mathbb{E}_\rho\left[Z\left(\rho\right)^n\right] = \int \prod_{\alpha=1}^{n} \mathrm{d}\mathbf{v}^{(\alpha)}\ \exp\left\{-\frac{\beta z}{2}\left(\mathbf{v}^{(\alpha)\dagger}\mathbf{v}^{(\alpha)} - nN\right) + \frac{\beta a_\eta}{2N}\mathbf{v}^{(\alpha)\dagger}\mathbf{u}\mathbf{u}^\dagger\mathbf{v}^{(\alpha)}\right\} \\ \prod_{\alpha=1}^{n}\mathbb{E}_{\xi^{(\alpha)}}\left[\exp\left\{\frac{\beta b_\eta}{2\left(P-1\right)}\sum_{\alpha,\beta}^{n}\xi^{(\alpha)}\mathbf{v}^{(\alpha)\dagger}\mathbf{v}^{(\beta)}\xi^{(\beta)}\right\}\right]^{P-1},\end{aligned} \tag{3.2.12}$$

where $\xi^{(\alpha)}$ is an auxiliary scalar field with the property $\xi^{(\alpha)} \overset{\text{i.i.d}}{\sim} \mathcal{N}\left(0,1\right)$ that was introduced via a Hubbard-Stratonovich transformation in order to linearize the quadratic disorder present in Eq. (3.2.11).

Something important to notice is that the previously independent replicas of the system have now been coupled together via the term $\propto \mathbf{v}^{(\alpha)\dagger}\mathbf{v}^{(\beta)}$. Such a coupling is always produced when one averages over the disorder and is in fact a very important quantity in every replica calculation as we will see now.

3.2.2 The replica order parameters

Looking at the form of Eq. 3.2.12 now motivates us to introduce the following overlap parameters

$$Q_{\alpha\beta} = \frac{1}{N}\mathbf{v}^{(\alpha)\dagger}\mathbf{v}^{(\beta)} \quad \text{and} \quad m_\alpha = \frac{1}{N}\mathbf{v}^{(\alpha)\dagger}\mathbf{u}, \tag{3.2.13}$$

where $\mathbf{Q} \in \mathbb{R}^{n\times n}$ and $\mathbf{m} \in \mathbb{C}^n$. In the theory of spin glasses, the first quantity $\mathbf{Q}$ is also referred to as the Edward-Anderson (EA) order parameter [40] essentially determining the overlap between different spin replicas of the system. Additionally, one can view $\mathbf{m}$ as an order parameter representing the magnetization of the system.

Plugging these two parameters back into our equations and performing the Gaussian integral over $\boldsymbol{\xi}$ then gives us (see Appendix B.1.2)

$$\begin{aligned}\mathbb{E}_\rho\left[Z\left(\rho\right)^n\right] = \int \prod_{\alpha=1}^{n} \mathrm{d}\mathbf{v}^{(\alpha)} \; \exp\left\{-\frac{N\beta z}{2}\left(\sum_{\alpha=1}^{n} Q_{\alpha\alpha} - n\right) + \frac{N\beta a_\eta}{2}\sum_{\alpha=1}^{n} m_\alpha m_\alpha^*\right\} \\ \exp\left\{-\frac{N\alpha}{2}\log\left[\det\left(\mathbf{I}_n - \frac{\beta b_\eta}{\alpha}\mathbf{Q}\right)\right]\right\}.\end{aligned} \tag{3.2.14}$$

As a next step in our calculations, we now want to perform the integration over the different replicas $\mathbf{v}^{(\alpha)}$. This poses a major challenge since formally we integrate over the hypersphere $\mathbb{S}^{N-1}\left(\sqrt{N}\right)$. To circumvent this problem, we can take use of the "Dirac-Fourier" method, which is essentially a trick to multiply our equations by one in a way to enforce the respective definitions of $\mathbf{Q}$ and $\mathbf{m}$. By then additionally demanding that the diagonal elements $Q_{\alpha\alpha} = 1$, we can extend the integral over $\mathbf{v}^{(\alpha)}$ to all of $\mathbb{R}^N$ since the δ-distributions will automatically enforce that $\mathbf{v}^{(\alpha)} \in \mathbb{S}^{N-1}\left(\sqrt{N}\right)$.

The "Dirac-Fourier" now works as follows. First, we write down the two resolution of identities:

$$1 = \int \mathrm{d}\mathbf{Q} \prod_{\alpha,\beta=1}^{n} \delta\left(Q_{\alpha\beta} - \frac{1}{N}\mathbf{v}^{(\alpha)\dagger}\mathbf{v}^{(\beta)}\right) = \int \mathrm{d}\mathbf{m} \prod_{\alpha=1}^{n} \delta\left(m_\alpha - \frac{1}{N}\mathbf{v}^{(\alpha)\dagger}\mathbf{u}\right).$$

Next, we replace the δ-distributions with their corresponding Fourier representations, these are

$$\begin{aligned}\delta\left(Q_{\alpha\beta} - \frac{1}{N}\mathbf{v}^{(\alpha)\dagger}\mathbf{v}^{(\beta)}\right) &= \int \frac{\mathrm{d}\hat{Q}_{\alpha\beta}}{(4\pi i/N)} \exp\left[\hat{Q}_{\alpha\beta}\left(\frac{N}{2}Q_{\alpha\beta} - \frac{1}{2}\mathbf{v}^{(\alpha)\dagger}\mathbf{v}^{(\beta)}\right)\right], \\ \delta\left(m_\alpha - \frac{1}{N}\mathbf{v}^{(\alpha)\dagger}\mathbf{u}\right) &= \int \frac{\mathrm{d}\hat{m}_\alpha}{(2\pi i/N)} \exp\left[\hat{m}_\alpha\left(Nm_\alpha - \mathbf{v}^{(\alpha)\dagger}\mathbf{u}\right)\right],\end{aligned}$$

where $\hat{Q}_{\alpha\beta}$ and $\hat{m}_\alpha$ are the conjugate variables of $Q_{\alpha\beta}$ and m_α respectively. Note that, in the above definitions, we absorbed a factor $2i/N$ into the definitions of the conjugate variables. Given that the integral will be dominated by the saddle point of the exponential term in the thermodynamic limit, we are free to drop such prefactors for the remaining part of the calculation to improve readability.

Inserting everything back into our equation for the average of the partition function

and rearranging some terms finally leaves us with the lengthy expression

$$\begin{aligned}\mathbb{E}_\rho\left[Z\left(\rho\right)^n\right] \simeq & \left(\int \prod_{\alpha,\beta=1}^{n} \mathrm{d}m_\alpha \mathrm{d}\hat{m}_\alpha \mathrm{d}Q_{\alpha\beta} \mathrm{d}\hat{Q}_{\alpha\beta}\right) \\ & \exp\left\{\frac{N}{2}\left(\sum_{\alpha,\beta=1}^{n} \hat{Q}_{\alpha\beta}Q_{\alpha\beta} + 2\sum_{\alpha=1}^{n} \hat{m}_\alpha m_\alpha + \beta a_\eta \sum_{\alpha=1}^{n} m_\alpha^2\right)\right\} \\ & \exp\left\{-\frac{N\alpha}{2}\log\left[\det\left(\mathbf{I}_n - \frac{\beta b_\eta}{\alpha}\mathbf{Q}\right)\right]\right\} \\ & \left(\int \prod_{\alpha=1}^{n} \mathrm{d}\mathbf{v}^{(\alpha)}\right) \exp\left\{-\frac{1}{2}\sum_{\alpha,\beta}^{n} \mathbf{v}^{(\alpha)\dagger}\hat{Q}_{\alpha\beta}\mathbf{v}^{(\beta)} - \sum_{\alpha=1}^{n} \hat{m}_\alpha \mathbf{v}^{(\alpha)\dagger}\mathbf{u}\right\},\end{aligned} \tag{3.2.15}$$

where we killed the term $\propto (\sum_{\alpha=1}^{n} Q_{\alpha\alpha} - n)$ since we already enforced $Q_{\alpha\alpha} = 1$.

We are now finally in a position to evaluate the integral over the different replicas $\mathbf{v}^{(\alpha)}$. One can show (again, see Appendix B.1.3 for a detailed derivation), that the result of the integral is given by

$$\exp\left\{\frac{N}{2}\left[n\log\left[2\pi\right] - \log\left[\det\left(\hat{\mathbf{Q}}\right)\right] + \sum_{\alpha,\beta=1}^{n} \hat{m}_\alpha \hat{Q}_{\alpha\beta}^{-1}\hat{m}_\beta\right]\right\}. \tag{3.2.16}$$

Finally, we are now able to collect all terms in the exponent into a single function and write

$$\mathbb{E}_\rho\left[Z\left(\rho\right)^n\right] \simeq \int \mathrm{d}\mathbf{m}\mathrm{d}\hat{\mathbf{m}}\mathrm{d}\mathbf{Q}\mathrm{d}\hat{\mathbf{Q}}\; e^{\frac{N}{2}\varphi\left(\mathbf{Q},\hat{\mathbf{Q}},\mathbf{m},\hat{\mathbf{m}}\right)}, \tag{3.2.17}$$

where the function φ is now given by

$$\begin{aligned}\varphi\left(\mathbf{Q},\hat{\mathbf{Q}},\mathbf{m},\hat{\mathbf{m}}\right) = & \sum_{\alpha,\beta=1}^{n} \hat{Q}_{\alpha\beta}Q_{\alpha\beta} + 2\sum_{\alpha=1}^{n} \hat{m}_\alpha m_\alpha + \beta a_\eta \sum_{\alpha=1}^{n} m_\alpha^2 \\ & - \alpha\log\left[\det\left(\mathbf{I}_n - \frac{\beta b_\eta}{\alpha}\mathbf{Q}\right)\right] + \sum_{\alpha,\beta=1}^{n} \hat{m}_\alpha \hat{Q}_{\alpha\beta}^{-1}\hat{m}_\beta \\ & - \log\left[\det\left(\hat{\mathbf{Q}}\right)\right] + n\log\left(2\pi\right).\end{aligned} \tag{3.2.18}$$

At present, the integral given by Eq. (3.2.17) does not seem to be analytically tractable. In order to still be able to evaluate it, we are going to take use of what is known as the "method of steepest-descent" in the literature. In its basic form (modulo prefactors) it states that [41]

$$\int \mathrm{d}x\; e^{-Mf(x)} \approx e^{-Mf(x_0)}, \quad \text{for} \quad M \to \infty,$$

and where x_0 denotes the minimum point of $f(x)$.

To justify the use of this method for our analysis, let us remind ourselves that we wanted to compute

$$\Phi = -\lim_{N\to\infty} \frac{2}{N}\mathbb{E}\left[\log\left(Z\right)\right] = -\lim_{N\to\infty} \frac{2}{N}\lim_{n\to 0} \frac{\mathbb{E}\left[Z^n\right] - 1}{n}.$$

The next step is mathematically not rigorous but a vital step in every replica calculation. Even though this may seem as a problem, as already mentioned above, if often still leads

to correct predictions that are in line with physical intuition and numerical simulations. Namely, we swap the order of the two limits above to get

$$\Phi = -\lim_{n\to 0}\frac{1}{n}\lim_{N\to\infty}\frac{2}{N}\mathbb{E}\left[Z^n\right].$$

Applying now Eq. (3.2.2) to our integral finally gives us

$$\Phi = -\lim_{n\to 0}\frac{1}{n}\text{extr}\left[\varphi\left(\mathbf{Q},\hat{\mathbf{Q}},\mathbf{m},\hat{\mathbf{m}},z\right)\right], \tag{3.2.19}$$

where extr $[\cdot]$ means, that we should evaluate φ at its saddle-point where

$$\frac{\partial\varphi}{\partial\mathbf{Q}}=0,\quad \frac{\partial\varphi}{\partial\hat{\mathbf{Q}}}=0,\quad \frac{\partial\varphi}{\partial\mathbf{m}}=0,\quad \frac{\partial\varphi}{\partial\hat{\mathbf{m}}}=0\quad\text{and}\quad \frac{\partial\varphi}{\partial z}=0. \tag{3.2.20}$$

3.2.3 The replica symmetric ansatz

While this extremization task may seem unfeasible in its current form, we can employ something known as the replica symmetric (RS)-ansatz in order to make it tractable. In this ansatz, one makes the reasonable assumption that at the extremum all the different replicas are equivalent, implying that the overlap $\mathbf{Q}$ between different replicas and the "magnetization" $\mathbf{m}$ will all concentrate on a single value. We thus parametrize these order parameters as

$$Q_{\alpha\beta} = (1-q)\,\delta_{\alpha\beta}+q, \tag{3.2.21}$$

$$\hat{Q}_{\alpha\beta} = \left(\hat{Q}-\hat{q}\right)\delta_{\alpha\beta}+\hat{q}, \tag{3.2.22}$$

$$m_\alpha = m\quad\text{and}\quad \hat{m}_\alpha=\hat{m}. \tag{3.2.23}$$

Using the RS-ansatz, we can now go back to Eq (3.2.18) and evaluate the corresponding terms. Doing this gives us (see for a detailed derivation)

$$\begin{aligned}\Phi = -\text{extr}\Bigg[\lim_{n\to 0}\frac{1}{n}\Bigg(&n^2q\hat{q}+n\left(\hat{Q}-q\hat{q}\right)+n2m\hat{m}+n\beta a_\eta m^2\\&-n\alpha\log\left[1-\frac{\beta b_\eta}{\alpha}(1-q)\right]-\alpha\log\left[1-\frac{n}{\alpha}\frac{q\beta b_\eta}{\left(1-\frac{\beta b_\eta}{\alpha}(1-q)\right)}\right]\\&-n\log\left[\hat{Q}-\hat{q}\right]-\log\left[1+n\frac{\hat{q}}{\hat{Q}-\hat{q}}\right]+n\log(2\pi)\\&+n\hat{m}^2(\gamma-\sigma)+n^2\hat{m}^2\sigma\Bigg)\Bigg],\end{aligned} \tag{3.2.24}$$

where the diagonal and off-diagonal elements of $\hat{\mathbf{Q}}^{-1}$ were respectively defined as (as derived in Appendix B.2.1)

$$\gamma=\frac{\hat{Q}+(n-2)\,\hat{q}}{\hat{Q}^2+(n-2)\,\hat{q}\hat{Q}-(n-1)\,\hat{q}^2}\quad\text{and}\quad \sigma=-\frac{\hat{q}}{\hat{Q}^2+(n-2)\,\hat{q}\hat{Q}-(n-1)\,\hat{q}^2}. \tag{3.2.25}$$

Note that we additionally swapped the order of the limit and the extremum in the expression for the free entropy above. This swap can be made rigorous if one first extremizes the function at finite n and then lets $n\to 0$.

With Eq. (3.2.24) at hand we are now in a good position to perform the analytic continuation of $n \to 0$. Using the fact that $\log(1-x) \approx -x + \mathcal{O}(x^2)$ for $x \ll 1$ then allows us to evaluate the limit as

$$\begin{aligned}\Phi = -\text{extr}\Bigg[&\hat{Q} - q\hat{q} + 2m\hat{m} + \beta a_\eta m^2 - \alpha \log\left[1 - \frac{\beta b_\eta}{\alpha}(1-q)\right] \\ &+ \frac{q\beta b_\eta}{\left(1 - \frac{\beta b_\eta}{\alpha}(1-q)\right)} - \log\left[\hat{Q} - \hat{q}\right] - \frac{\hat{q}}{\left(\hat{Q} - \hat{q}\right)} \\ &+ \frac{\hat{m}^2}{\left(\hat{Q} - \hat{q}\right)} + \log[2\pi]\Bigg],\end{aligned}$$

which now got transformed into a manageable optimization problem over 5 scalar variables.

3.2.4 Minimizing the free entropy

Let us start this optimization task by minimizing Φ w.r.t. $\hat{q}$. After some simple algebra we arrive at

$$q = -\frac{1}{\left(\hat{Q} - \hat{q}\right)^2}\left[\hat{q} - \hat{m}^2\right]. \tag{3.2.26}$$

On the other hand, minimization w.r.t. $\hat{Q}$ gives us

$$1 - \frac{1}{\hat{Q} - \hat{q}} = -\frac{1}{\left(\hat{Q} - \hat{q}\right)^2}\left[\hat{q} - \hat{m}^2\right],$$

which, combined with Eq. (3.2.26), implies that

$$\hat{Q} - \hat{q} = \frac{1}{1-q}. \tag{3.2.27}$$

In order to simplify the following calculations, we now collect all the terms we have evaluated so far and plug them back into Φ. To do so, we take use of the expression above while also expressing $\hat{q}$ as a function of q and $\hat{m}^2$ using Eq. (3.2.26). Doing all this, then leads us to

$$\begin{aligned}\Phi = -\text{extr}\Bigg[&2m\hat{m} + \beta a_\eta m^2 + \hat{m}^2(1-q) + \log[2\pi] + \frac{1}{(1-q)} \\ &-\alpha \log\left[1 - \frac{\beta b_\eta}{\alpha}(1-q)\right] + \frac{q\beta b_\eta}{\left(1 - \frac{\beta b_\eta}{\alpha}(1-q)\right)} + \log[1-q]\Bigg].\end{aligned} \tag{3.2.28}$$

What remains now is only the optimization over the variables $\hat{m}$, m and q. It is easy to confirm the minimization w.r.t. to the former gives us the condition that

$$\hat{m} = -\frac{m}{1-q}.$$

Inserting this expression back into Φ then gives us the following simplified form of the free entropy

$$\Phi = -\text{extr}\left[\log\left[1-q\right] + \frac{1-m^2}{(1-q)} + \beta a_\eta m^2 + \log\left[2\pi\right] \right. \\ \left. -\alpha \log\left[1 - \frac{\beta b_\eta}{\alpha}(1-q)\right] + \frac{q\beta b_\eta}{\left(1-\frac{\beta b_\eta}{\alpha}(1-q)\right)}\right]. \tag{3.2.29}$$

This allows us now to easily compute the derivative w.r.t. to m and set it to zero. This hands us the condition that

$$m\left(\beta a_\eta - \frac{1}{(1-q)}\right) \stackrel{!}{=} 0, \tag{3.2.30}$$

while the optimization w.r.t. to q gives us

$$\frac{q-m^2}{(1-q)^2} = \frac{1}{\alpha}\frac{q\beta^2 b_\eta^2}{\left(1-\frac{\beta b_\eta}{\alpha}(1-q)\right)^2}.$$

Using the fact that Eq. (3.2.30) can only have non-zero solutions for m if $\beta a_\eta = (1-q)^{-1}$, then allows us to derive an expression for the overlap squared, namely

$$m^2 = q\left(1 - \frac{\alpha b_\eta^2}{(\alpha a_\eta - b_\eta)^2}\right)$$

We will now argue that for $m^2 \neq 0$, we can expect the replica overlap q to be positive and equal to 1 since the replicas become increasingly aligned with their preferred direction $\mathbf{u}$. This will already pave us the way to retrieve the critical parameters of the model, since it means that we can have only non-negative solutions for m^2 if

$$\frac{\alpha b_\eta^2}{(\alpha a_\eta - b_\eta)^2} < 1, \tag{3.2.31}$$

from which η_c and α_c can be extracted.

To verity the statement above, let us compute the EA order parameter q. We start with the condition that is given to us by Eq. (3.2.30). Inserting this expression back into Φ, lets us conclude that the free entropy can be written as

$$\Phi = -\text{extr}\left[\log\left[1-q\right] + \frac{1}{(1-q)} - \alpha\log\left[1-\frac{\beta b_\eta}{\alpha}(1-q)\right] \right. \\ \left. + \frac{q\beta b_\eta}{\left(1-\frac{\beta b_\eta}{\alpha}(1-q)\right)} + \log\left[2\pi\right]\right]. \tag{3.2.32}$$

Taking the derivative w.r.t. q and setting it zero this time gives us

$$\frac{q}{(1-q)^2} = \frac{1}{\alpha}\frac{q\beta^2 b_\eta^2}{\left(1-\frac{\beta b_\eta}{\alpha}(1-q)\right)^2},$$

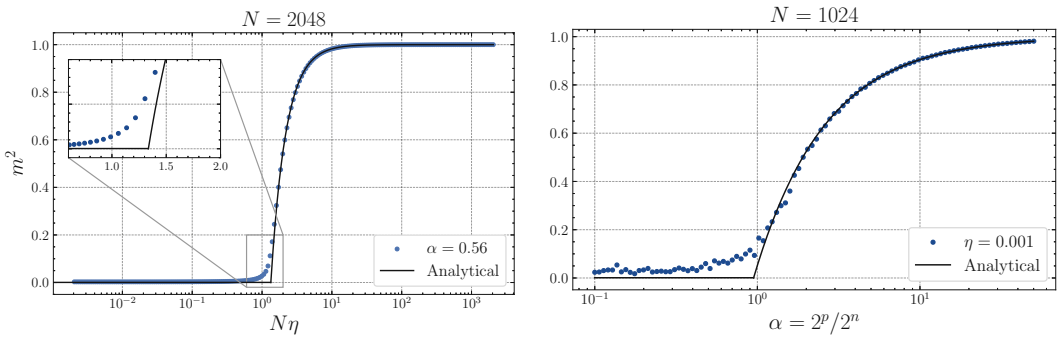

(a) (b)

Figure 3.2: Squared overlap between our trajectory **u** and the most probable state of the evolved density matrix ρ. The simulations were performed for a system of $n = 11$ and $n = 10$ spin-1/2 particles respectively. We averaged over a total of 50 runs. The inset in (a) highlights the N^{-1} dependence of the critical value of η.

which is just a quadratic equation in q that can be easily solved.

We differentiate now between two cases. For $\alpha = 1$, the quadratic equation above has the two easy solutions

$$q_0 = 0, \quad \text{and} \quad q_1 = 1 - \frac{1}{2\beta b_\eta}.$$

In the second case, where $\alpha \neq 1$, it can be easily shown that the two solutions are given by

$$q_\pm = 1 - \frac{1}{\beta b_\eta} \frac{\alpha}{1 \pm \sqrt{\alpha}}.$$

Since we have that β, b_η and α are strictly positive, we have that all solutions fulfil the physical intuitive condition that $q \leq 1, \forall \alpha \geq 0$. Since, however, only solution q_+ matches with q_1 in the case when $\alpha = 1$, we pick q_+ as our physically relevant result for the replica overlap q, i.e. we have

$$q = 1 - \frac{1}{\beta b_\eta} \frac{\alpha}{1 + \sqrt{\alpha}}.$$

Remember that the interest for our model is given by the region where we let $\beta \to \infty$ since only then the replica vector **v** will condense onto the groundstate of our effective Hamiltonian. We thus justified the statement we made above since $q \to 1$ in this limit.

This now allows us to write m^2 as function of η and α alone and brings us to the final result

$$m^2 = 1 - \frac{\alpha b_\eta^2}{(\alpha a_\eta - b_\eta)^2}. \tag{3.2.33}$$

Given the form of the parameters a_η and b_η (Eqs. (3.2.2) and (3.2.3)) and in a setting where N and P are sufficiently large enough, this function will be well approximated by

$$m^2 \approx 1 - \frac{\alpha (1-\eta)^2}{(N\alpha\eta - (1-\eta))^2}. \tag{3.2.34}$$

Furthermore, returning to Eq. (3.2.31), lets us conclude that we can expect a phase transition in the retrievability of our trajectory at the critical value

$$\eta_c = \frac{1 + \sqrt{\alpha} - \frac{\alpha N}{\alpha N - 1}}{1 + \sqrt{\alpha} + N\alpha}, \tag{3.2.35}$$

which, in the limit where $P = \alpha N$ becomes large enough, is well approximated by

$$\eta_c \approx \frac{1}{N\sqrt{\alpha}}. \tag{3.2.36}$$

As can be seen in Fig. 3.2a above, we have a good agreement between our analytically derived result for m^2 and numerical simulations.

Further, one can now rearrange Eq. (3.2.35) in order to retrieve the critical value of α. Since the full solution well be given by an extremely lengthy polynomial (solvable via any numerical software of your choice), we make the approximation that in the large P limit we have $P/(P-1) \approx 1$, which leads us to

$$\alpha_c \approx \frac{1}{2\eta^2 N^2}\left[J(\eta, N) + \sqrt{K(\eta, N)}\right], \tag{3.2.37}$$

where

$$J(\eta, N) = 1 - 2\eta + \eta^2 - 2\eta^2 N,$$
$$K(\eta, N) = \left(2\eta^2 N - \eta^2 + 2\eta - 1\right)^2 - 4\eta^4 N^2.$$

Again, we check the validity of this result by comparing it to numerical simulation in Fig. 3.2b. Apart from the finite-size effects that appear in a region where $\alpha \ll 1$, we again have a very good fit of our analytical derived result with the simulations. We want to note that these finite size effects are completely natural since our assumptions about very large values of P do not hold in the relevant region.

Below we also plot the phase diagram of our model for a specific range of α. Note that because of the N^{-1} scaling of η_c, we already a see a transition to the retrievable phase for very low values of η.

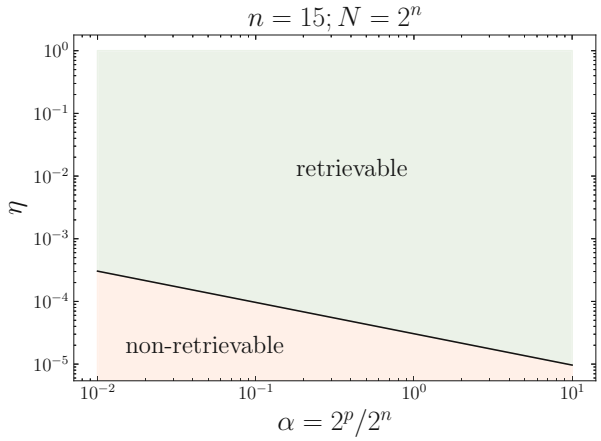

Figure 3.3: Phase diagram for a system of $n = 15$ spin-1/2 particles, corresponding to a system Hilbert space dimension of $N = 2^{15}$ and an environment with p particles corresponding to a dimension of $P = 2^p$. The green and the red region depict the retrievable and the non-retrievable phases of our system respectively. Parameter pairs (η, α) lying inside the green region indicate that the evolved ρ contains enough information to reconstruct the trajectory $\mathbf{u}$.

CHAPTER 4

Conclusion and outlook

In this thesis we explored the dynamics of open quantum many-body systems under continuous measurements and the emergent phenomena resulting from the interplay between quantum trajectories and decoherence. By employing a simplified model of interacting particles, we interpolated between the extremes of fully retaining or fully discarding the measurement results. We demonstrated a sharp transition between a regime where a single trajectory could be reconstructed from the backdrop of purely dissipative dynamics. Using tools from RMT, quantum information theory, and spin glass theory, we derived analytical expressions for the order parameters of the model and identified their critical values. We further checked the validity of our calculations by comparing the analytical results to numerical simulations and found a very good fit.

While this work primarily focused on the behavior of the system over a single discrete time step, future research should extend the analysis to dynamics over arbitrarily long times. A key question to address is whether the sharp transition observed in this short-term dynamics persists or vanishes over time. Understanding the stability of the retrievable phase during extended evolution would provide valuable insight into the nature of these transitions. Additionally, determining whether the long-term behavior of the system can be described analytically, or if the complexities of extended dynamics require alternative approaches, poses an intriguing challenge.

Finally, as continuously monitored quantum systems become increasingly experimentally viable, examining the long-term interplay between trajectories and decoherence may have vital impact on the design of robust quantum computing and simulation platforms.

APPENDIX A

Random quantum channels

A.1 Random quantum channel constitutes a POVM

As mentioned, we want to show that the POVM, defined by the Kraus operators in Equation (2.2.1), satisfies, on average, the resolution of identity condition while also being self-averaging. This means we have to show that

$$\mathbb{E}[M] = \mathrm{I}_N, \quad \text{with} \quad M = \sum_{n=1}^{P} A_n^\dagger A_n, \tag{A.1.1}$$

and

$$\mathrm{Var}[M] = \mathbb{E}\left[M^2\right] - (\mathbb{E}[M])^2 = \frac{q}{N}\mathrm{I}_N. \tag{A.1.2}$$

The proof goes as follows:

Proof A.1.1

$$\begin{aligned}
\mathbb{E}[M_{ij}] &= \mathbb{E}\left[\sum_{n=1}^{P}\sum_{k=1}^{N}\langle i|A_n^\dagger|k\rangle\langle k|A_n|j\rangle\right] \\
&= \sum_{n=1}^{P}\sum_{k=1}^{N}\mathbb{E}\left[(A_n)_{ki}^\dagger (A_n)_{kj}\right] \\
&= \frac{1}{NP}\sum_{n=1}^{P}\sum_{k=1}^{N}\mathbb{E}\left[(G_n)_{ki}^\dagger (G_n)_{kj}\right] \\
&= \frac{1}{NP}\sum_{n=1}^{P}\sum_{k=1}^{N}\delta_{ij} \\
&= \delta_{ij} = (\mathrm{I})_{ij}\,.
\end{aligned} \tag{A.1.3}$$

While, by using the fact that $\left(\sum_n^P a_n\right)^2 = \sum_{n,m}^P a_n a_m$, we have for the mean of M^2

$$\begin{aligned}
\mathbb{E}\left[\left(M^2\right)_{ij}\right] &= \mathbb{E}\left[\sum_{n,m}^{P}\sum_{a,b,c}^{N}\langle i|A_n^\dagger|a\rangle\langle a|A_n|b\rangle\langle b|A_m^\dagger|c\rangle\langle c|A_m|j\rangle\right] \\
&= \frac{1}{N^2P^2}\sum_{n,m}^{P}\sum_{a,b,c}^{N}\mathbb{E}\left[(G_n)^\dagger_{ai}(G_n)_{ab}(G_n)^\dagger_{cb}(G_n)_{cj}\right] \\
&= \frac{1}{N^2P^2}\sum_{n,m}^{P}\sum_{a,b,c}^{N}\left[\delta_{ib}\delta_{bj}+\delta_{nm}\delta_{ac}\delta_{ij}\right] \\
&= \left(1+\frac{1}{P}\right)\delta_{ij} = \left(1+\frac{q}{N}\right)(\mathrm{I}_N)_{ij}\,,
\end{aligned} \tag{A.1.4}$$

where Wicks' theorem [42] was used to arrive at the third line. Combining this with the result obtained in Equation (A.1.3) completes our proof. □

A.2 State preparation through random channel

Here we show the self-averaging property of the quantity p_m, i.e. that the following holds:

$$\mathbb{E}\left[p_m\right] = \frac{1}{P}, \tag{A.2.1}$$

and

$$\mathrm{Var}\left[p_m\right] = \mathbb{E}\left[p_m^2\right] - \left(\mathbb{E}\left[p_m\right]\right)^2 = \frac{q^2}{N^3}. \tag{A.2.2}$$

The proof goes as follows.

Proof A.2.1

We start by calculating the average, namely

$$\begin{aligned}
\mathbb{E}\left[p_m\right] &= \mathbb{E}\left[\mathrm{tr}\left(A_m\rho_S A_m^\dagger\right)\right] \\
&= \frac{1}{NP}\mathbb{E}\left[\sum_{n=1}^{N}\langle n|G_m|0\rangle\langle 0|G_m^\dagger|n\rangle\right] \\
&= \frac{1}{NP}\sum_{n=1}^{N}\mathbb{E}\left[G_{m,n0}G_{m,0n}^\dagger\right] \\
&= \frac{1}{P}.
\end{aligned} \tag{A.2.3}$$

Next, we show that the average of the square is equal to

$$\begin{aligned}\mathbb{E}\left[p_m^2\right] &= \mathbb{E}\left[\mathrm{tr}\left(A_m \rho_S A_m^\dagger\right)^2\right] \\ &= \frac{1}{N^2P^2}\sum_{i,j}^{N}\mathbb{E}\left[G_{m,i0}G_{m,0i}^\dagger G_{m,j0}G_{m,0j}^\dagger\right] \\ &= \frac{1}{N^2P^2}\sum_{i,j}^{N}(1+\delta_{ij}) \\ &= \frac{1}{P^2}+\frac{1}{NP^2} = \frac{1}{P^2}+\frac{q^2}{N^3},\end{aligned} \tag{A.2.4}$$

where we defined the quantity $q = N/P$. □

To show that the state prepared by the measurement is indeed properly normalized on average, we want to derive

$$\mathbb{E}\left[\langle\psi|\psi\rangle\right] = 1 \tag{A.2.5}$$

and

$$\mathrm{Var}\left[\langle\psi|\psi\rangle\right] = \frac{1}{N}. \tag{A.2.6}$$

Proof A.2.2

The first property is easy, using the definition of c_j given in Equation (2.2.10), we have

$$\mathbb{E}\left[\langle\psi|\psi\rangle\right] = \sum_{j=1}^{N}\mathbb{E}\left[c_j^* c_j\right] = \sum_{j=1}^{N}\frac{1}{N} = 1. \tag{A.2.7}$$

For the second property, we will write the coefficient c_n as

$$c_j = \mathrm{Re}\left(G_{m,j0}\right) + i\,\mathrm{Im}\left(G_{m,j0}\right) = x_j + iy_j, \tag{A.2.8}$$

with

$$\mathbb{E}\left[x_j^2\right] = \mathbb{E}\left[y_j^2\right] = \sigma^2 = \frac{1}{2N}. \tag{A.2.9}$$

This allows us to compute the average of the squared norm as

$$\begin{aligned}\mathbb{E}\left[\langle\psi|\psi\rangle^2\right] &= \sum_{n,m}^{N}\mathbb{E}\left[c_n^* c_n c_m^* c_m\right] \\ &= \sum_{n,m}^{N}\mathbb{E}\left[x_n^2 x_m^2\right] + \mathbb{E}\left[y_n^2 y_m^2\right] + \mathbb{E}\left[x_n^2 y_m^2\right] + \mathbb{E}\left[y_n^2 x_m^2\right] \\ &= \sum_{n=1}^{N}\mathbb{E}\left[x_n^4\right] + \mathbb{E}\left[y_n^4\right] + 2\mathbb{E}\left[x_n^2\right]\mathbb{E}\left[y_n^2\right] + \sum_{n\neq m}^{N}\mathbb{E}\left[x_n^2 x_m^2\right] + \dots \\ &= \sum_{n=1}^{N} 3\sigma^4 + 3\sigma^4 + 2\sigma^4 + \sum_{n\neq m}^{N}\sigma^4 + \sigma^4 + \sigma^4 + \sigma^4 \\ &= 1 + \frac{1}{N},\end{aligned} \tag{A.2.10}$$

completing our proof. □

APPENDIX B

The replica calculation

B.1 Computing the free entropy

Lets us provide in a bit more detail how one can compute the average given by

$$\mathbb{E}_{\mathbf{G}}\left[\exp\left\{\frac{\beta b_\eta}{2\left(P-1\right)}\sum_{\alpha=1}^{n}\sum_{\mu=1}^{P-1}\mathbf{v}^{(\alpha)\dagger}\mathbf{g}_\mu\mathbf{g}_\mu^\dagger\mathbf{v}^{(\alpha)}\right\}\right], \tag{B.1.1}$$

such that it leads to the final result

$$\left[\prod_{\alpha=1}^{n}\mathbb{E}_{\xi^{(\alpha)}}\left[\exp\left\{\frac{\beta b_\eta}{2\left(P-1\right)}\sum_{\alpha,\beta}^{n}\xi^{(\alpha)}\mathbf{v}^{(\alpha)\dagger}\mathbf{v}^{(\beta)}\xi^{(\beta)}\right\}\right]\right]^{P-1}. \tag{B.1.2}$$

Calculation B.1.1

First note that Eq. (B.1.1) can be rewritten to

$$\begin{aligned}&\prod_{\mu=1}^{P-1}\mathbb{E}_{\mathbf{g}_\mu}\left[\exp\left\{\frac{\beta b_\eta}{2\left(P-1\right)}\sum_{\alpha=1}^{n}\left(\mathbf{v}^{(\alpha)\dagger}\mathbf{g}_\mu\right)^2\right\}\right]\\ =&\prod_{\mu=1}^{P-1}\mathbb{E}_{\mathbf{g}_\mu}\left[\prod_{\alpha=1}^{n}\mathbb{E}_{\xi^{(\alpha)}}\left[\exp\left\{\xi^{(\alpha)}\left(\sqrt{\frac{\beta b_\eta}{P-1}}\mathbf{v}^{(\alpha)\dagger}\mathbf{g}_\mu\right)\right\}\right]\right],\end{aligned} \tag{B.1.3}$$

where $\xi^{(\alpha)} \overset{\text{i.i.d}}{\sim} \mathcal{N}\left(0,1\right)$ is the aforementioned auxiliary scalar field introduced by the Hubbard-Stratonovich transformation. That the second equality holds can be easily seen by observing that for a standard Gaussian random variable x we have

$$\mathbb{E}_x\left[\exp\left\{bx\right\}\right] = \exp\left\{\frac{b^2}{2}\right\}. \tag{B.1.4}$$

Now that we have linearized the quantity that we are averaging over, we can safely perform the Gaussian integral over the disorder by remembering that the

elements $(\mathbf{g}_\mu)_i \overset{\text{i.i.d}}{\sim} \mathcal{N}(0,1)$ to get

$$\left[\prod_{\alpha=1}^{n} \mathbb{E}_{\xi^{(\alpha)}}\left[\exp\left\{\frac{\beta b_\eta}{2(P-1)}\left(\sum_{\alpha=1}^{n} \mathbf{v}^{(\alpha)\dagger}\xi^{(\alpha)}\right)^2\right\}\right]\right]^{P-1}. \tag{B.1.5}$$

Finally, by again using the relation that $\left(\sum_n^P a_n\right)^2 = \sum_{n,m}^P a_n a_m$, we arrive at Eq. (B.1.2) which is what we wanted to show.

Next, we want to incorporate the order parameter $\mathbf{Q}$ into Eq. 3.2.12 and show that it give us

$$\exp\left\{-\frac{N\alpha}{2}\log\left[\det\left(\mathbf{I}_n - \frac{\beta b_\eta}{\alpha}\mathbf{Q}\right)\right]\right\}. \tag{B.1.6}$$

Calculation B.1.2

As a first step, we can plug in the definition of the order parameter $\mathbf{Q}$ to Eq. (B.1.2) to arrive at

$$\left[\prod_{\alpha=1}^{n} \mathbb{E}_{\xi^{(\alpha)}}\left[\exp\left\{\frac{\beta b_\eta}{2\alpha}\sum_{\alpha,\beta}^{n}\xi^{(\alpha)}Q_{\alpha\beta}\xi^{(\beta)}\right\}\right]\right]^{P}. \tag{B.1.7}$$

Note that since we are only interested in the large P limit, we made the approximation $P-1 \approx P$. Explicitly writing the Gaussian integral over the random variable $\boldsymbol{\xi} \in \mathbb{R}^n$ then gives us

$$\left[\frac{1}{\sqrt{(2\pi)^n \det(\mathbf{I}_n)}}\int \mathrm{d}\boldsymbol{\xi}\exp\left\{-\frac{1}{2}\boldsymbol{\xi}^\top\left(\mathbf{I}_n - \frac{\beta b_\eta}{\alpha}\mathbf{Q}\right)\boldsymbol{\xi}\right\}\right]^{P}, \tag{B.1.8}$$

Finally, doing the standard Gaussian integral then gives us

$$\det\left(\mathbf{I}_n - \frac{\beta b_\eta}{\alpha}\mathbf{Q}\right)^{-\frac{P}{2}}, \tag{B.1.9}$$

which can be readily rewritten in the form of Eq. (B.1.6).

We now want to compute the integral over the different replicas $\mathbf{v}^{(\alpha)}$ in Eq. (3.2.15) and show that the result is given by

$$\exp\left\{\frac{N}{2}\left[n\log[2\pi] - \log\left[\det\left(\hat{\mathbf{Q}}\right)\right] + \sum_{\alpha,\beta=1}^{n}\hat{m}_\alpha\hat{Q}^{-1}_{\alpha\beta}\hat{m}_\beta\right]\right\}. \tag{B.1.10}$$

Calculation B.1.3

We begin by reminding the reader that at the beginning of our calculations, we choose the special representation for our trajectory $\mathbf{u} = \left(\sqrt{N}, 0, \ldots, 0\right)^\top$. What this essentially means is, that the dot product in the exponent $\mathbf{v}^{(\alpha)\dagger}\mathbf{u}$ will always pick out the first component of the vector $\mathbf{v}$. The integral over all N components of the replicas $\mathbf{v}^{(\alpha)}$ thus essentially decouples into a product of $N-1$ integrals

over the last $N-1$ components and one integral over the first component of $\mathbf{v}^{(\alpha)}$. Written down explicitly, this means that we can write

$$\left[\int \mathrm{d}\mathbf{v} \exp\left\{-\frac{1}{2}\mathbf{v}^\dagger \hat{\mathbf{Q}}\mathbf{v}\right\}\right]^{N-1} \int \mathrm{d}\mathbf{v} \exp\left\{-\frac{1}{2}\mathbf{v}^\dagger \hat{\mathbf{Q}}\mathbf{v} - \sqrt{N}\hat{\mathbf{m}}^\dagger \mathbf{v}\right\}, \tag{B.1.11}$$

where one has to be careful since $\mathbf{v} \in \mathbb{R}^n$ now. The result of both integrals can be obtained by the standard Gaussian integral which states that

$$\int \mathrm{d}\mathbf{x} \exp\left\{-\frac{1}{2}\mathbf{x}^\dagger \mathbf{A}\mathbf{x} + \mathbf{B}^\dagger \mathbf{x}\right\} = \sqrt{\frac{(2\pi)^n}{\det(A)}} \exp\left\{\frac{1}{2}\mathbf{B}^\dagger \mathbf{A}^{-1}\mathbf{B}\right\}. \tag{B.1.12}$$

Lastly, it just remains to identify $\mathbf{B} = 0$ for the first $N-1$ integrals and $\mathbf{B}^\dagger = -\sqrt{N}\mathbf{m}^\dagger$ for the remaining integral to arrive at the form given by Eq. (B.1.10).

B.2 The free entropy under replica symmetry

Here we want to provide a detailed derivation on how to arrive at the free entropy given by Eq. (3.2.24) under the assumption of RS. For this, we start with function Φ as given in Eq. (3.2.18) and examine the corresponding terms one by one.

Calculation B.2.1

Calculating the first term under replica symmetry (Eqs. (3.2.21) to (3.2.23)) is easy and gives us

$$\sum_{\alpha,\beta}^{n} \hat{Q}_{\alpha\beta} Q_{\alpha\beta} = n^2 q\hat{q} + n\left(Q\hat{Q} - q\hat{q}\right). \tag{B.2.1}$$

For the terms that contain the logarithm of the determinant we can take use of the determinant lemma which states that [43]

$$\det\left(\mathbf{A} + \mathbf{u}\mathbf{v}^\top\right) = \left(1 + \mathbf{v}^\top \mathbf{A}^{-1}\mathbf{u}\right)\det(\mathbf{A}). \tag{B.2.2}$$

To apply this method to our expressions, we explicitly rewrite the term containing $\det(\mathbf{I}_n - b_\eta/\alpha \mathbf{Q})$ to

$$\log\left[\det\left(\left(1 - \frac{\beta b_\eta}{\alpha}(Q-q)\right)\mathbf{1}_n - \frac{q\beta b_\eta}{\alpha}\mathbf{d}\mathbf{d}^\top\right)\right], \tag{B.2.3}$$

where, $\mathbf{d} = (1,1,\ldots,1)^\top \in \mathbb{R}^n$. Straightforward application of the determinant lemma then gives us

$$n\log\left[1 - \frac{\beta b_\eta}{\alpha}(Q-q)\right] + \log\left[1 - \frac{n}{\alpha}\frac{q\beta b_\eta}{\left(1 - \frac{\beta b_\eta}{\alpha}(Q-q)\right)}\right]. \tag{B.2.4}$$

Equivalently, the term containing $\det\left(\hat{\mathbf{Q}}\right)$ leads to

$$n\log\left[\hat{Q} - \hat{q}\right] + \log\left[1 + n\frac{\hat{q}}{\hat{Q} - \hat{q}}\right]. \tag{B.2.5}$$

The last non-trivial term remaining is now the expression containing the inverse of $\hat{\mathbf{Q}}$. As already state, we claim that the inverse can be parameterized by

$$\hat{Q}^{-1}_{\alpha\beta} = (\gamma - \sigma)\,\delta_{\alpha\beta} + \sigma, \tag{B.2.6}$$

where γ and σ are given by Eq. (3.2.25). This result can be proven with the well-known Sherman-Morrison formula [44], which states that the inverse of a matrix given by the sum $\mathbf{A} + \mathbf{u}\mathbf{v}^\top$, where $\mathbf{A} \in \mathbb{R}^{n\times n}$ and $\mathbf{v}, \mathbf{u} \in \mathbb{R}^n$, can be written as

$$\left(\mathbf{A} + \mathbf{u}\mathbf{v}^\top\right)^{-1} = \mathbf{A}^{-1} - \frac{\mathbf{A}^{-1}\mathbf{u}\mathbf{v}^\top\mathbf{A}^{-1}}{1 + \mathbf{v}^\top\mathbf{A}^{-1}\mathbf{u}}. \tag{B.2.7}$$

Rewriting $\hat{\mathbf{Q}}$ into

$$\hat{\mathbf{Q}} = \left(\hat{Q} - \hat{q}\right)\mathbf{I}_n + \hat{q}\mathbf{d}\mathbf{d}^\top, \tag{B.2.8}$$

then directly leads to the desired result that

$$\hat{\mathbf{Q}}^{-1} = \frac{1}{\left(\hat{Q} - \hat{q}\right)}\mathbf{I}_n - \frac{1}{\left(\hat{Q} - \hat{q}\right)^2}\frac{\hat{q}}{\left(1 + \frac{n\hat{q}}{\left(\hat{Q} - \hat{q}\right)}\right)}\mathbf{d}\mathbf{d}^\top. \tag{B.2.9}$$

With this expression at hand one can directly read of the diagonal elements γ and off-diagonal elements σ after a bit of simple algebra.

Bibliography

[1] D. A. Abanin, E. Altman, I. Bloch, and M. Serbyn, "Colloquium: Many-body localization, thermalization, and entanglement", Reviews of Modern Physics **91**, 021001 (2019).

[2] M. Rigol, V. Dunjko, and M. Olshanii, "Thermalization and its mechanism for generic isolated quantum systems", Nature **452**, 854–858 (2008).

[3] H.-P. Breuer and F. Petruccione, *The Theory of Open Quantum Systems*, 1st ed. (Oxford University PressOxford, Jan. 25, 2007).

[4] A. J. Leggett, S. Chakravarty, A. T. Dorsey, M. P. A. Fisher, A. Garg, and W. Zwerger, "Dynamics of the dissipative two-state system", Reviews of Modern Physics **59**, 1–85 (1987).

[5] C. Gardiner and P. Zoller, *Quantum Noise: A Handbook of Markovian and Non-Markovian Quantum Stochastic Methods with Applications to Quantum Optics* (Springer Science & Business Media, Aug. 27, 2004), 476 pp.

[6] H. A. Weidenmüller, "Quantum Chaos, Random Matrices, and Irreversibility in Interacting Many-Body Quantum Systems", Entropy **24**, 959 (2022).

[7] P. O'Donovan, P. Strasberg, K. Modi, J. Goold, and M. T. Mitchison, *Quantum master equation from the eigenstate thermalization hypothesis*, (Nov. 12, 2024) `http://arxiv.org/abs/2411.07706`, pre-published.

[8] D. W. Leung, "Quantum computation by measurements", International Journal of Quantum Information **02**, 33–43 (2004).

[9] D. A. Lidar and T. A. Brun, eds., *Quantum Error Correction* (Cambridge University Press, Cambridge, 2013).

[10] H. J. Carmichael and K. Kim, "A quantum trajectory unraveling of the superradiance master equation1", Optics Communications **179**, 417–427 (2000).

[11] M. P. Fisher, V. Khemani, A. Nahum, and S. Vijay, "Random Quantum Circuits", Annual Review of Condensed Matter Physics **14**, 335–379 (2023).

[12] A. J. Daley, "Quantum trajectories and open many-body quantum systems", Advances in Physics **63**, 77–149 (2014).

[13] Y. Li, X. Chen, and M. P. A. Fisher, "Measurement-driven entanglement transition in hybrid quantum circuits", Physical Review B **100**, 134306 (2019).

[14]B. Skinner, J. Ruhman, and A. Nahum, "Measurement-Induced Phase Transitions in the Dynamics of Entanglement", Physical Review X **9**, 031009 (2019).

[15]J. M. Koh, S.-N. Sun, M. Motta, and A. J. Minnich, "Measurement-induced entanglement phase transition on a superconducting quantum processor with mid-circuit readout", Nature Physics **19**, 1314–1319 (2023).

[16]Y. Li, X. Chen, and M. P. A. Fisher, "Quantum Zeno effect and the many-body entanglement transition", Physical Review B **98**, 205136 (2018).

[17]A. Chan, R. M. Nandkishore, M. Pretko, and G. Smith, "Unitary-projective entanglement dynamics", Physical Review B **99**, 224307 (2019).

[18]S. Lloyd, M. Mohseni, and P. Rebentrost, "Quantum principal component analysis", Nature Physics **10**, 631–633 (2014).

[19]E. Tang, "Quantum Principal Component Analysis Only Achieves an Exponential Speedup Because of Its State Preparation Assumptions", Physical Review Letters **127**, 10.1103/PhysRevLett.127.060503 (2021).

[20]B. Skinner, *Lecture Notes: Introduction to random unitary circuits and the measurement-induced entanglement phase transition*, (July 6, 2023) http://arxiv.org/abs/2307.02986, pre-published.

[21]P. Hayden and J. Preskill, "Black holes as mirrors: quantum information in random subsystems", Journal of High Energy Physics **2007**, 120 (2007).

[22]Y. Sekino and L. Susskind, "Fast scramblers", Journal of High Energy Physics **2008**, 065 (2008).

[23]*Quantum Noise: A Handbook of Markovian and Non-Markovian Quantum Stochastic Methods with Applications to Quantum Optics | SpringerLink*, https://link.springer.com/book/9783540223016.

[24]J. Ginibre, "Statistical Ensembles of Complex, Quaternion, and Real Matrices", Journal of Mathematical Physics **6**, 440–449 (1965).

[25]C. Mastrodonato and R. Tumulka, "Elementary Proof for Asymptotics of Large Haar-Distributed Unitary Matrices", Letters in Mathematical Physics **82**, 51–59 (2007).

[26]D. Petz and J. Réffy, "On asymptotics of large Haar distributed unitary matrices", Periodica Mathematica Hungarica **49**, 103–117 (2004).

[27]J. Wishart, "The Generalised Product Moment Distribution in Samples from a Normal Multivariate Population", Biometrika **20A**, 32–52 (1928).

[28]V. A. Marčenko and L. A. Pastur, "Distribution of Eigenvalues for some Sets of Random Matrices", Mathematics of the USSR-Sbornik **1**, 457–483 (1967).

[29]J. Baik, G. B. Arous, and S. Péché, "Phase transition of the largest eigenvalue for nonnull complex sample covariance matrices", The Annals of Probability **33**, 1643–1697 (2005).

[30]P. Reimann, C. V. D. Broeck, and G. J. Bex, "A Gaussian scenario for unsupervised learning", Journal of Physics A: Mathematical and General **29**, 3521–3535 (1996).

[31]P. Reimann and C. Van Den Broeck, "Learning by examples from a nonuniform distribution", Physical Review E **53**, 3989–3998 (1996).

[32]T. L. H. Watkin and J.-P. Nadal, "Optimal unsupervised learning", Journal of Physics A: Mathematical and General **27**, 1899 (1994).

[33]V. Chandrasekaran, B. Recht, P. A. Parrilo, and A. S. Willsky, "The Convex Geometry of Linear Inverse Problems", Foundations of Computational Mathematics **12**, 805–849 (2012).

[34]D. O. Hebb, *The organization of behavior; a neuropsychological theory*, The Organization of Behavior; a Neuropsychological Theory (Wiley, Oxford, England, 1949), pp. xix, 335, xix, 335.

[35]E. Oja, "Simplified neuron model as a principal component analyzer", Journal of Mathematical Biology **15**, 267–273 (1982).

[36]J. Baik and J. O. Lee, "Fluctuations of the Free Energy of the Spherical Sherrington–Kirkpatrick Model", Journal of Statistical Physics **165**, 185–224 (2016).

[37]D. Sherrington and S. Kirkpatrick, "Solvable Model of a Spin-Glass", Physical Review Letters **35**, 1792–1796 (1975).

[38]J. J. Hopfield, "Neural networks and physical systems with emergent collective computational abilities", Proceedings of the National Academy of Sciences of the United States of America **79**, 2554 (1982).

[39]G. Parisi, "Infinite Number of Order Parameters for Spin-Glasses", Physical Review Letters **43**, 1754–1756 (1979).

[40]S. F. Edwards and P. W. Anderson, "Theory of spin glasses", Journal of Physics F: Metal Physics **5**, 965 (1975).

[41]H. Huang, in *Statistical Mechanics of Neural Networks* (Springer Nature Singapore, Singapore, 2021), pp. 71–72.

[42]G. C. Wick, "The Evaluation of the Collision Matrix", Physical Review **80**, 268–272 (1950).

[43]D. A. Harville, *Matrix Algebra From a Statistician's Perspective* (Springer, New York, NY, 1997).

[44]J. Sherman and W. J. Morrison, "Adjustment of an Inverse Matrix Corresponding to a Change in One Element of a Given Matrix", The Annals of Mathematical Statistics **21**, 124–127 (1950).

Glossary

BBP Baik-Ben Arous-Péché 9

EA Edward-Anderson 16, 20

PCA Principal Component Analysis 2, 13

POVM positive operator-valued measure 4, 7, 24

RMT random matrix theory 2, 6, 23

RS replica symmetric 18, 29

SK Sherrington-Kirkpatrick 12, 15

SSK spherical Sherrington-Kirkpatrick 11